



Cite this: *Dalton Trans.*, 2014, **43**, 12943

Kinetics and mechanistic investigation into the possible activation of imidazolium *trans*-[tetrachloridodimethylsulfoxideimidazole-ruthenate(III)], NAMI-A, by 2-mercaptoethane sulfonate†

Risikat Ajibola Adigun,^a Bice Martincigh,^b Vincent O. Nyamori,^b Bernard Omondi,^b Collen Masimirembwa^c and Reuben H. Simoyi^{*a,b}

Imidazolium *trans*-[tetrachloridodimethylsulfoxideimidazole-ruthenate(III)], NAMI-A, is a promising anti-metastatic prodrug with high specificity for metastatic cancer cells. Limited activity of NAMI-A against primary tumor suggests that its use in combination with other anticancer drug(s) might present a more desirable therapeutic outcome. The mechanism of activation and action of this prodrug is still largely unknown. The biological targets, as well, have not yet been delineated. The kinetics and mechanism of interaction of NAMI-A with 2-mercaptoethane sulfonate, MESNA, a chemoprotectant, have been studied spectrophotometrically under pseudo-first order conditions of excess MESNA. The reaction is characterized by initial reduction of NAMI-A and formation of dimeric MESNA as evidenced by electrospray ionization mass spectrometry. A first order dependence on both NAMI-A and MESNA was obtained and a bimolecular rate constant of $0.71 \pm 0.06 \text{ M}^{-1} \text{ s}^{-1}$ was deduced. Activation parameters determined ($\Delta S^\ddagger = -178.12 \pm 0.28 \text{ J K}^{-1} \text{ mol}^{-1}$, $\Delta H^\ddagger = 20.64 \pm 0.082 \text{ kJ mol}^{-1}$ and $\Delta G^\ddagger = 75.89 \pm 1.76 \text{ kJ mol}^{-1}$ at $37 \pm 0.1 \text{ }^\circ\text{C}$ and pH 7.4) are indicative of formation of an associative intermediate prior to product formation and subsequent hydrolysis of the reduced complex. Our results suggest that MESNA might be able to activate the prodrug while still protecting against toxicity when given in a regimen involving NAMI-A and chemotherapy drug(s) that induce bladder and kidney toxicities.

Received 4th June 2014,
Accepted 22nd June 2014

DOI: 10.1039/c4dt01643b

www.rsc.org/dalton

Introduction

Despite all the years spent studying cancer cures, to date, the most common way to cure cancer is to remove or block the fast proliferating malignant tissues.¹ The promising results obtained in the clinical treatment of some tumors with *cis*-diammine-dichloroplatinum(II) (cisplatin) have unleashed many studies directed towards inorganic compounds of platinum and other metals in an attempt to improve therapeutic activity on tumors.^{2–5} Cisplatin was the first inorganic compound developed which was able to block DNA replication and cell division,

opening up a new research section on metallopharmaceuticals.⁶ The major disadvantage of major metal-based antineoplastic drugs in present use; cisplatin, is the high and unacceptable levels of nephrotoxicity,^{7–9} neurotoxicity^{10–14} and eventual development of drug resistance.^{15–22} Current research in metal-based chemotherapeutic agents is focused on improving pharmacological profiles of a series of possible non-platinum-based anticancer agents.²³

Recently, most studies into further inorganic metal-based antineoplastic drugs have focused on ruthenium complexes. There has been essentially an exponential growth in the number of publications in the past ten years dealing with the synthesis of ruthenium-based anticancer drugs.^{24–26} There have also been several review articles highlighting the properties of this class of antineoplastic compounds, stressing the differences that characterize ruthenium compounds *versus* those of platinum and other transition metals.^{27–29} A number of these novel ruthenium compounds have demonstrated significant cytotoxic and antimetastatic properties with low levels of side effects. Two particularly promising drug candidates; Imidazolium

^aDepartment of Chemistry, Portland State University, Portland, OR 97207-0751, USA. E-mail: rsimoyi@pdx.edu

^bSchool of Chemistry, University of KwaZulu-Natal Westville Campus, Private Bag X54001, Durban 4000, Republic of South Africa

^cAfrican Institute of Biomedical Science and Technology, P.O. Box 2294, Harare, Zimbabwe

†Electronic supplementary information (ESI) available. See DOI: 10.1039/c4dt01643b

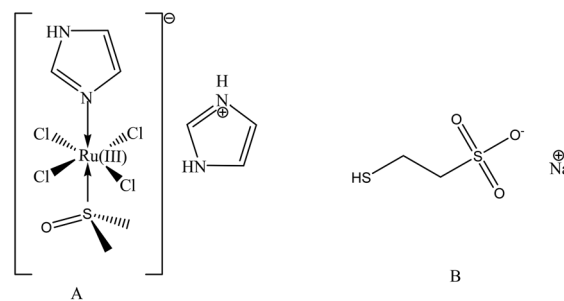
trans-[tetrachloridodimethylsulfoxideimidazole]ruthenate(III) (NAMI-A) and indazolium *trans*-[tetrachlorobis(1*H*-indazole)-ruthenate(III)] (KP1019) have successfully completed phase I clinical trials and are undergoing further clinical evaluation.^{30–32}

These ruthenium compounds have given the medical community hope that anticancer drugs may be derived that are significantly more effective *versus* the existing platinum drugs with their disadvantage of low activity coupled with high toxicity.^{8,18,33}

NAMI-A, is an experimental prodrug that shows low host toxicity and selectively targets metastatic cells.^{32,34–36} NAMI-A, while being very active against metastases has relatively limited activity towards primary tumor.^{26,37} This suggests that administration of NAMI-A in combination with drug(s) active against primary tumor might present a more desirable chemotherapy outcome. Renal failure, however, in cancer patients is a common problem in oncology and this complication is frequently multifactorial in origin. Several antineoplastic agents are potentially nephrotoxic, and combinations with other nephrotoxic drugs will increase the risk of nephrotoxicity during administration of chemotherapy.^{38–40} Cisplatin nephrotoxicity is clearly dose-related and is now considered to be the dose-limiting factor in the absence of chemoprotectants.⁴¹ Most anticancer drugs and their metabolites are eliminated through the kidneys, thus, making the kidneys susceptible to injury.⁴²

A combination, therefore, of NAMI-A and any other anticancer drugs will require a concurrent use of a chemoprotectant to prevent nephrotoxicity. Chemoprotection aims at prevention, mitigation or delay of toxicity, thus increasing therapeutic index of chemotherapy without interfering with efficacy of applied drug.⁴³ This is expected to improve a patient's quality of life. Failure to provide adequate chemoprotection during therapy may mandate withdrawal or postponement of treatment and consequently lowers the probability of treatment success.

Sodium-2-mercaptoethanesulfonate, MESNA (MesnexTM), is a low molecular weight thiol in clinical use as a chemoprotectant to inhibit the hemorrhagic cystitis and prevent bladder and kidney toxicities induced by cisplatin, ifosfamide and cyclophosphamide.^{41,44–46} Mesna for i.v. administration was initially approved by the FDA in 1988, and the oral formulation in 2002.⁴⁷ Successful Phase II clinical trials have already been performed on the prophylactic use of Mesnex for women receiving a regimen of carboplatin and ifosfamide for advanced breast cancer carcinomas.⁴⁸ This current clinical utility of MESNA suggests that an encounter with NAMI-A will be inevitable should NAMI-A be used as part of a combination regimen involving any nephrotoxic cancer drug. A recent study reports on cancer cure in 60% of animals treated for lung metastasis using a combination of cisplatin and NAMI-A in mouse models.⁴⁹ This represents the most successful treatment reported for metastasis.⁵⁰ It therefore becomes essential to investigate the interactions of NAMI-A that are important for optimizing its clinical use with MESNA at high dosages of nephrotoxic agents.



(A) Imidazolium *trans*-tetrachloro(dimethyl sulfoxide)imidazole- ruthenate(III), NAMI-A

(B) Sodium 2-mercaptoethane sulfonate

Here, we present a first report on kinetics and mechanism of interaction of NAMI-A with MESNA under physiologically-relevant conditions. NAMI-A is co-injected with MESNA in any therapy regimen. What is the effect of MESNA on the efficacy of NAMI-A? What are the kinetics factors involved in this interaction? The most commonly accepted mechanism for the activity of Ru(III) anticancer agents involves ligand exchange with serum components, followed by cellular uptake.⁵¹ Ruthenium is up-taken as Ru(III), while the anti-cancer form is the Ru(II) state.⁵² MESNA, as a reducing thiol, should readily interact with NAMI-A, and possibly reduce its efficacy(?). Final safe dosages for both NAMI-A and MESNA should account for this interaction. An understanding of this interaction is expected to provide information useful for the design of chemotherapy regimen involving a combination of NAMI-A and any anticancer drugs that induce bladder or kidney toxicity for improved treatment outcome.

Materials and methods

Materials

MESNA and other chemicals were of analytical grade, purchased from commercial sources and used as obtained. Distilled deionized water obtained from a Barnstead NANO pure water purification unit was used to prepare solutions and buffers. The pH of the solutions was measured with a 720 A+, Thermo-Orion pH meter. Phosphate or acetate buffer was used to adjust pH of the experimental solutions. Reactions were carried out at 25.0 ± 0.1 °C (except when isolating the effect of temperature) and at a constant ionic strength of 1.0 M using NaClO₄.

Hydrogen *trans*-bis(dimethyl sulfoxide)tetrachlororuthenate (III), the precursor for NAMI-A, was synthesized using a published literature method.³⁶ NAMI-A was synthesized from this precursor. 0.49 g of imidazole was added to 1.0 g of precursor suspended in 20 mL of acetone at room temperature. This mixture was stirred for 4 hours. The precipitate obtained in this manner was washed with cold acetone and ethyl ether. Characterization of this complex was done using UV/VIS, NMR and electrospray ionization mass spectrometry (ESI-MS). Spectral data were in good agreement with those reported in literature.⁵³

Instrumentation/methods

UV/Vis spectral data were recorded using a Perkin-Elmer Lambda 25 UV/Vis spectrophotometer. ^1H NMR data were obtained from a 400 MHz Bruker NMR spectrometer. Mass spectral data of product solutions were obtained using a Thermo-Scientific LTQ-Orbitrap Discovery mass spectrometer (San Jose, CA) equipped with electrospray ionization source operated in the negative mode. Reaction kinetics were studied by monitoring the consumption of NAMI-A at 390 nm ($\epsilon_{\text{H}_2\text{O}} = 3790 \pm 56 \text{ M}^{-1} \text{ cm}^{-1}$) using a Hi-Tech ScientificTM SF-61DX2 stopped flow spectrophotometer. Initial rates are presented as average of at least 3–5 kinetic runs.

Results and discussion

Product identification. Fig. 1 shows the spectral changes observed from a solution of MESNA and NAMI-A scanned at 30 second intervals. The charge transfer band of NAMI-A at 390 nm decreased as reaction progressed, indicating a one-electron reduction of NAMI-A. The shoulder at 345 nm initially increased and then decreased towards the end of reaction. Absence of an isosbestic point indicates involvement of other absorbing species. Reduced form of NAMI-A, $[\text{ImRuCl}_4\text{DMSO}]^{2-}$, has been reported to have a half life of approximately 14 s.⁵⁴ Upon formation, it is expected that this labile species will be rapidly hydrolyzed in the prevailing aqueous reaction conditions. A full electro-spray ionization mass spectrum of the stoichiometric solution was taken in the negative mode within the first minute of reaction (Fig. 2a). The spectrum features NAMI-A at $m/z = 390$ (exact: 389.83) and MESNA at $m/z = 141$ (exact: 140.97) as being the most abundant. A small peak at $m/z = 139.96$ represents the already formed disulfide of MESNA. As expected, no peak was observed for the reduced NAMI-A at $m/z = 194$ since it is known to be extremely labile. Spectrum in

Fig. 2b, taken five minutes after Fig. 2a shows decrease in both NAMI-A and MESNA peaks with simultaneous growth of the disulfide of MESNA. Fig. 2c, taken at 5 minutes later shows the disulfide as most abundant, demonstrating the progression of the reaction towards completion. Spectrum 2b shows the decomposition pathway of the complex. The decrease in the NAMI-A peak centered at m/z 389 gives a peak at m/z 321 which shows an initial loss of the imidazole ligand before loss of the DMSO ligand. The peaks centered at m/z 243 indicate the ruthenium center, still in the +3 state and having lost both apical ligands, $[\text{RuCl}_4]^-$. The Ruthenium(II) complex would show up at m/z approximately 121. There was no strong peak observed at this value. There was also no sign of the octahedral diaquo-tetrachloro complex, $[\text{RuCl}_4(\text{H}_2\text{O})_2]^-$, expected at about 277; suggesting that the ruthenium complex, upon losing the two apical ligands, remained strictly square planar. Mass spectral data analysis strongly suggest that the UV-Vis 345 nm transient peak should be from the 5-coordinate ruthenium species centered at m/z 321. UV-Vis spectral data had shown a transient peak at 345 nm as a shoulder of the dominant 390 nm peak.

Reaction stoichiometry. The only oxidation product observed in excess of MESNA over NAMI-A is the dimeric disulfonate $^- \text{O}_3\text{SCH}_2\text{CH}_2\text{S}-\text{SCH}_2\text{CH}_2\text{SO}_3^-$. This product was proved by NMR spectroscopy. MESNA, in D_2O gave an NMR spectrum with two triplet peaks, one centered at 2.80 ppm and the other at 3.11 ppm. After oxidation by NAMI-A, the NMR spectrum showed only one coalesced singlet peak at 3.17 ppm since all 8 protons in the disulfonate become equivalent. This reduces to a 1:2 stoichiometry of MESNA to complex. The expected reduction product, after prolonged standing, with ruthenium in the d-6 +2 oxidation state would be in the hexaquo form, $\text{Ru}(\text{H}_2\text{O})_6^{2+}$. The d-6 electronic configuration cannot support a square planar geometry of RuCl_4^{2-} . The ultimate form of the Ru(II) complex could not be determined since several hydrated and hydroxylated combinations could be obtained and have been detected by NMR techniques in previous studies.⁵¹

Kinetics

NAMI-A dependence. Effect of varying initial concentrations of NAMI-A on the reaction in 0.1 M phosphate buffer at pH 7.4 was examined (see ESI Fig. S1†). The initial rate of consumption of NAMI-A increased with increasing initial NAMI-A concentrations. Absorbance traces at 390 nm in this figure (and all other subsequent traces which monitor consumption of NAMI-A) show what might appear, erroneously, as mild autocatalysis. The peak at 390 nm is not entirely isolated and is influenced by contribution from 345 nm, which appears as a shoulder to 390 nm peak (see Fig. 1). Since the peak at 345 nm initially increases, one would expect a positive contribution to the absorbance observed at 390 nm, from this peak. As the reaction proceeds, however, the peak at 345 nm starts to fall, with a concomitant decrease in its contribution at 390 nm. Thus the observed rate of decrease of the peak at 390 nm will be enhanced, without necessarily an increased decrease in rate of loss of NAMI-A. There is no stoichiometric link between

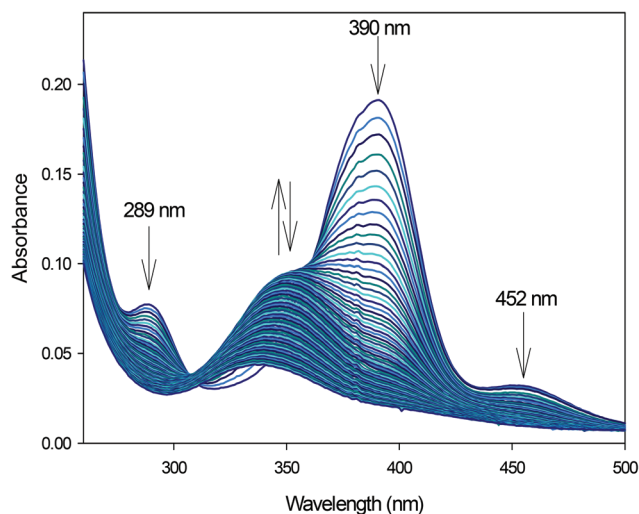


Fig. 1 Rapid spectral scan of aqueous solution of MESNA and NAMI-A taken at 30 s interval. $[\text{MESNA}]_0 = 1.5 \times 10^{-4} \text{ M}$; $[\text{NAMI-A}]_0 = 5.0 \times 10^{-5} \text{ M}$.

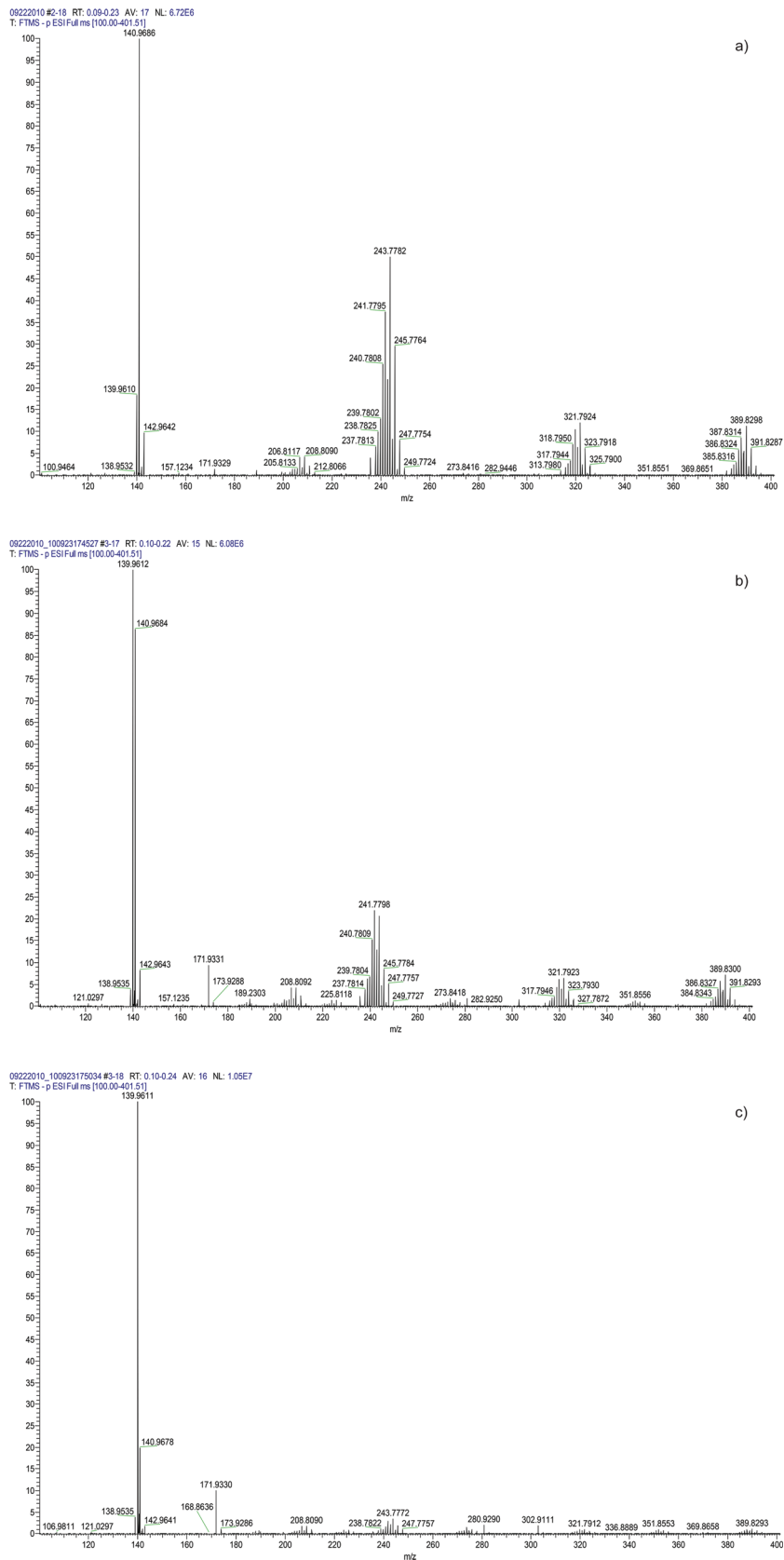


Fig. 2 (a) Negative ESI-MS spectrum of a stoichiometric solution of MESNA and NAMI-A within the first minute of the start of reaction. (b) Negative ESI-MS spectrum of the same solution in (a) taken five minutes later showing the consumption of both NAMI-A peak at 389.8300 m/z and MESNA peak at 140.9684 m/z with simultaneous growth of disulfide of MESNA at 139.9612 m/z and decay of MESNA. (c) Negative ESI-MS spectrum of solution in (a) taken ten minutes later showing disulfide of MESNA as the major peak.

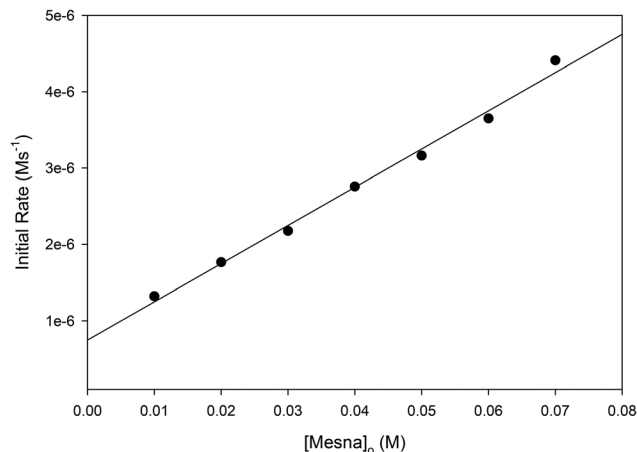


Fig. 3 Initial rate plot, showing linear dependence on MESNA. The positive intercept value indicates another route not mediated by MESNA.

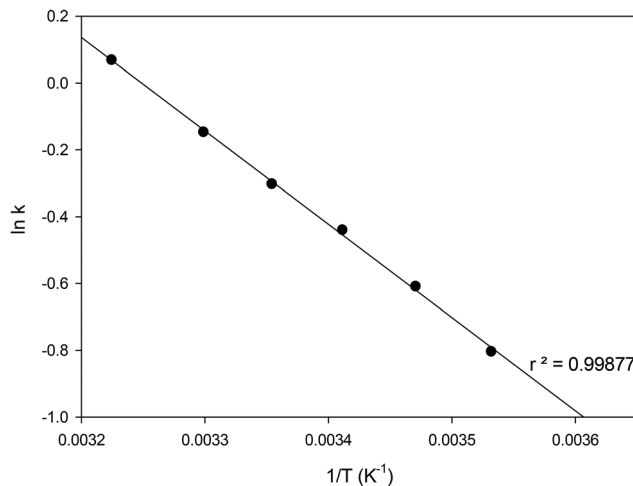


Fig. 4 Arrhenius plot extracted from study of effect of temperature variation on the reaction for the determination of activation parameters.

NAMI-A and the intermediate that absorbs at 345 nm, thus initial rates for all our kinetics determinations were confined to a very short initial part of the reaction before establishment of intermediates. Plot of initial rates against initial NAMI-A concentrations gave a straight line, with an intercept kinetically indistinguishable from zero, suggesting a linear dependence on NAMI-A (ESI Fig. S2†). A bimolecular rate constant of $7.07 \times 10^{-1} \pm 0.06 \text{ M}^{-1} \text{ s}^{-1}$ was deduced from these data. Due to the qualitative nature of the absorbance readings and initial contributions from the 345 nm peak, this bimolecular rate constant can only be considered as a lower-limit rate constant.

Since NAMI-A has been reported to be more stable at low pH,⁵⁵ influence of reduced pH on bimolecular rate constant was also evaluated (compare ESI Fig. S1 and S3†). The kinetics data show that, under similar conditions, reaction is almost twice as fast at pH 7.4 than it is at pH 6.0, proving that lower pH conditions enhance stability of the complex. The effect of varying initial NAMI-A concentrations were also evaluated at pH 6.0, separately, in 0.10 M acetate (ESI Fig. S3†) and 0.10 M phosphate (data not shown) buffer solutions as a way of evaluating whether the type of buffer anions has any effect on the rate or mechanism of reduction of NAMI-A. Comparison of these traces shows that no difference in reaction dynamics is observed with phosphate and when acetate anions are used for the buffer. These traces could be superimposed on each other with no distinguishability. This shows that intervention of the buffer ions is not involved in the rate determining step of reduction of NAMI-A.

MESNA dependence. Effect of variation of initial concentrations of MESNA was also monitored at 390 nm. The reaction rate monotonically increased with increasing concentrations of MESNA with no apparent saturation (ESI Fig. S4†). Initial rate plots deduced from this plot, again, show a linear first-order dependence on MESNA concentrations (see Fig. 3). This plot shows a positive intercept at zero concentrations of MESNA, indicating existence of other decomposition pathways that are not mediated by MESNA. These routes are assumed to

be the normal slow decomposition pathways of NAMI-A in aqueous conditions.

Temperature dependence. At constant ionic strength, concentrations of NAMI-A and MESNA, the effect of temperature on the reaction was evaluated. Reaction rate increased proportionally with increasing temperatures as expected from standard Arrhenius kinetics (see Fig. S5†), suggesting the existence of a dominant rate-determining step. The obtained data were used to construct an Arrhenius plot (see Fig. 4). Activation parameters deduced using information obtained from the Arrhenius plot are: entropy of activation, $\Delta S^\ddagger = -178.12 \pm 0.28 \text{ J K}^{-1} \text{ mol}^{-1}$, enthalpy of activation, $\Delta H^\ddagger = 20.64 \pm 0.082 \text{ kJ mol}^{-1}$ and free energy of activation as $\Delta G^\ddagger = 75.89 \pm 1.76 \text{ kJ mol}^{-1}$ at $37 \pm 0.1 \text{ }^\circ\text{C}$ and pH 7.4. The distinctly negative entropy of activation suggests some degree of molecular ordering in the rate determining step. These parameters are indicative of an associative mechanism.

Mechanism

This reaction was followed through color changes. Color changes indicate the change of a chromophore. All NAMI-A solutions, upon prolonged standing, in the presence or absence of a reductant, darken in color. From the work of Sava *et al.*, darkening to the brownish color is ascribed to the poly-oxo or hydroxyl species,⁵⁶ while a basic loss of color is ascribed to reduction of the ruthenium center from Ru(III) to Ru(II) (d^5 to d^6 configurations).⁵⁷ Our experimental observations were confined to the initial loss of color stage only, before extensive formation of poly-oxo species.

The observed kinetics data indicate a complex mechanism with a multi-term rate law. Reactions monitored with variation of ionic strength showed an enhancement of the rate of reduction of NAMI-A by MESNA with ionic strength; indicating that one of the rate-limiting steps involves a reaction between like charges or between dipoles. The Arrhenius plots data suggest an associative mechanism which involves adduct

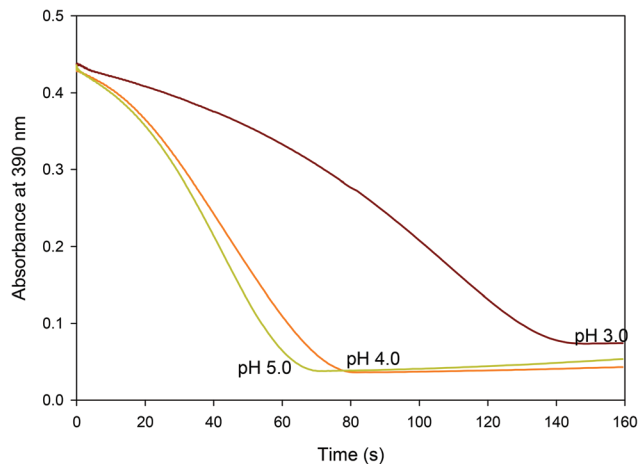
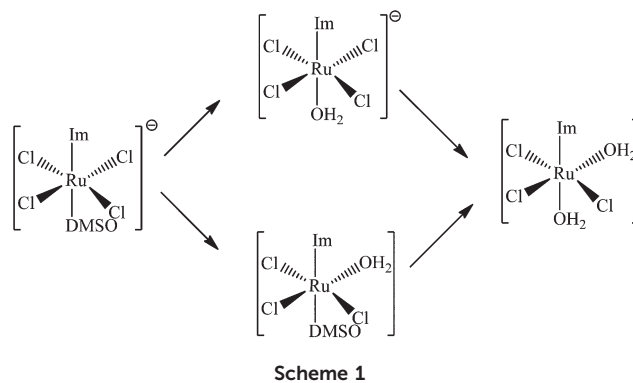


Fig. 5 Influence pH on reaction rate. Reaction in 0.1 M phosphate buffered at pH 3.0 proceeded slowly compared to pH 4.0 and 5.0. $[NAMI-A]_0 = 1.0 \times 10^{-4}$ M; $[MESNA]_0 = 5.0 \times 10^{-2}$ M.

formation in the rate-determining step (*vide supra*). Combining these results with the sluggishness of the reaction at lower pH conditions suggests that the thiolate anion of MESNA is its reactive form in the reduction of NAMI-A. Fig. 5 clearly shows the effect of pH on the rate of reaction, in which the rate progressively increases from pH 3 to 5. The disappearance of NAMI-A involves at least three major separate pathways. One pathway involves its own first order decomposition, k_0 . NAMI-A is most stable between pH 4 and 5, where it has a decomposition half-life of about 60 hours. It is least stable at pH 9 with a half-life of a few minutes. pH conditions utilized for these series of kinetics investigations were in the range of 3 to 7. This pathway is significant, as can be seen from MESNA dependence data (Fig. 3). This plot shows, from the non-zero intercept, a measurable decomposition rate of NAMI-A in the absence of MESNA. The next decomposition pathway involved the buffer anions, k_B . A study by Bouma *et al.*⁵⁵ showed that, while the half-life for the decomposition of NAMI-A is 66.6 hours in 0.01 M buffer, it plummets to 13.3 hours in 1.0 M buffer. The third route involves its reduction by MESNA, k_M . Our kinetics data show a linear relationship between MESNA concentrations and its rate of disappearance. This also shows that, within the range of MESNA concentrations shown, the rate of reaction is first order with respect to MESNA concentrations. The simple kinetics dependences with respect to MESNA and NAMI-A suggest dominance of the MESNA-mediated decomposition of NAMI-A over the other two pathways at the conditions applied for this series of kinetics studies. The speciation of NAMI-A itself, in the absence of reductant, is highly disputed, with various authors suggesting different possible pathways.^{58–60} These disputes, however, are strictly related to reaction conditions used. For example, reaction conditions utilizing NaCl *vs.* NaClO₄ to maintain ionic strength would deliver different decomposition mechanisms, rates and products since high chloride concentrations stabilize the complex from an initial loss of the equatorial chlorides

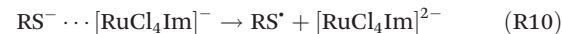
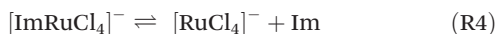


and instead releases the DMSO ligand first.⁵¹ The decomposition mechanism and subsequent species generated is strongly correlated with its antitumor activity because the active species should arise from these metabolites since the original NAMI-A complex itself is known to be inert and is activated by its reduction and/or hydrolysis to active form(s).^{51,52,61} In order to understand the coordination of NAMI-A to biological targets, a necessary prerequisite is a clear understanding of the stability and hydrolytic transformations of NAMI-A in aqueous solutions because an understanding of these processes is the crucial step in identifying the active species and evaluating their mode of interaction with DNA and other biological targets such as HSA.⁶⁰ By utilizing EPR activity of the low-spin ($s = 1/2$) Ru(III) complex (the corresponding Ru(II) species is EPR-silent),⁶² a recent EPR-based study on the ligand-exchange processes of NAMI-A complex in buffer and in presence of human serum albumin gave evidence for the most plausible decomposition pathway for the complex.⁵¹ This study observed an initial relatively rapid exchange of the DMSO ligand with a water molecule, a process that proceeds simultaneously with a slower exchange of one of the equatorial chlorides with water. This complex decomposition results in five other mononuclear ruthenium complexes which, after 24 hours and more, will give way to polynuclear oxo-bridged Ru(III) oligomers. This general decomposition scheme is represented as Scheme 1.

A comparable ¹H NMR-based study by Bacac⁶⁰ *et al.* also showed, at physiological pH, the simultaneous replacement of the equatorial Cl⁻ with water and displacement of the DMSO ligand, but their study showed that aquation of the equatorial chloride is faster than the displacement of the DMSO ligand. This happens within 15 minutes, while, at pH 3.0 the decomposition is much slower (*circa* 100 minutes), with only the DMSO ligand being pulled off. Our experimental data on the decomposition of NAMI-A in the presence of MESNA shows a slightly different decomposition scheme (see Fig. 2a–c), albeit faster than the rates of pure hydrolysis displayed by the complex itself in buffer and pH 7.4. Our experimental results agree with a cyclic voltammetry-cum-ESI-MS spectra experimental data⁵⁹ from Ravera *et al.* that show the initial removal of the imidazole ligand before the DMSO. Ravera's data involve the speciation pattern for NAMI-A under

MALDI-Q-ToF and in the absence of a reductant. Thus the $\text{RuCl}_4\text{DMSO}^-$ and RuCl_4^- complexes are reversibly attainable. Since this rate is faster in the presence of MESNA, one concludes that the reverse order of the removal of the axial ligands is mediated by MESNA. The series of Fig. 2a, b and c show the sequence of events in the reduction/activation of NAMI-A by MESNA: Fig. 2a is obtained soon after mixing NAMI-A and MESNA. It clearly shows the original NAMI-A at the expected $m/z = 390$ as well as the complex obtained after a loss of the imidazole ligand, $[\text{RuCl}_4(\text{DMSO})]^-$ at $m/z = 322$ and the square planar tetrachlororuthenate complex, $[\text{RuCl}_4]^-$. A large peak for MESNA at $m/z = 141$ is observed and a smaller peak for its oxidized form, the dimer, at $m/z = 140$. After an incubation time of 5 minutes, shown in Fig. 2b, the dimer peak increases at the expense of the monomer while all the other 3 peaks for the ruthenium complexes decrease. After 15 minutes, the reaction would have nearly gone to completion (Fig. 2c), two of the complexes are completely consumed with a small amount of the tetrachloro-complexes which is equivalent to the remaining MESNA which has not yet been converted to its dimer. Our ESI-MS experiments (Fig. 2a–c) were performed at stoichiometric ratios of 1 : 2 MESNA to NAMI-A; such that at the end of the reaction both complex and MESNA will be depleted with quantitative formation of the dimeric species. We note, here, that no electron transfer occurs during formation of the two ruthenium complexes upon addition of MESNA to NAMI-A. Formation of a Ru(II) complex would give different m/z values; which, in this case, would be 195, 162 and 122 respectively for $[\text{RuCl}_4(\text{DMSO})(\text{Im})]^{2-}$, $[\text{RuCl}_4(\text{DMSO})]^{2-}$ and $[\text{RuCl}_4]^{2-}$. None of these peaks were observed. The correlation between disappearance of the tetrachloro complex and the appearance of the dimer, suggests that oxidation of MESNA is dominated by the square planar $[\text{RuCl}_4]^-$ and not by the inert NAMI-A itself. Direct electron transfer from NAMI-A, the inert octahedral complex, would be outer-sphere; with a small negative entropy of activation value. The large negative entropy of activation derived in this reaction implicates an inner-sphere mechanism which involves large geometrical changes in the transition state.

An inclusive mechanism would involve the following series of reactions, R1–R13 and acidity equilibrium reaction of the thiol, K_a . The list involves all four possible oxidizing species: $[\text{ImRuCl}_4\text{DMSO}]^-$, $[\text{RuCl}_4\text{DMSO}]^-$, $[\text{RuCl}_4\text{Im}]^-$ and $[\text{RuCl}_4]^-$ oxidizing solely the thiolate anion, RS^- to give the thiyl radical. The thiyl radicals then combine to form the dimeric product of MESNA.



All the one-electron decomposition products; $[\text{ImRuCl}_4\text{DMSO}]^{2-}$, $[\text{RuCl}_4\text{DMSO}]^{2-}$ and $[\text{RuCl}_4]^{2-}$ rapidly hydrolyze to Ru(II) complexes of varying ligand substitutions. Our experimental data (Fig. 2a–c) indicate the dominance of the following reactions: R1, R2, R7 + R8, R11 + R12 and R13. This is the only plausible pathway that supports first order kinetics in MESNA.

The proposed mechanism suggests a strictly one-electron oxidation which results in thiyl radicals. Our e-scan EPR spectrometer, however, did not pick up thiyl radicals in the reaction mixture. There are also many buffer anions in solutions that could mask the possibility of secondary radicals such as the superoxide anion radicals that can be derived from the thiyl radicals in the aerobic environment utilized. The inertness of the d^5 octahedral geometry coupled with the strong associative thermodynamics parameters of the intermediate state strongly suggest that reactions R5 + R6 do not contribute to the overall reaction. None of the expected intermediates derived from the R5 + R6 sequence were observed on the mass spectrometer. The disruption of the octahedral symmetry is known to be a prerequisite for reactivity of NAMI-A. Since the active form of NAMI-A is the Ru(II) form, co-injection of MESNA with NAMI-A does not deactivate NAMI-A. The product of oxidation of MESNA, the dimeric form, $\text{BNP7787}^{\text{TM}}$,^{43,63,64} has been evaluated as a much better nephroprotectant than MESNA itself.⁶⁵

Acknowledgements

This work was supported by Grant Number CHE 1056311 from the National Science Foundation Catalysis Program; and a partial research professorship grant from the University of KwaZulu-Natal.

References

- 1 E. M. Nagy, C. Nardon, L. Giovagnini, L. Marchio, A. Trevisan and D. Fregona, *Dalton Trans.*, 2011, **40**, 11885.
- 2 E. Alessio, G. Mestroni, A. Bergamo and G. Sava, *Curr. Top. Med. Chem.*, 2004, **4**, 1525.

- 3 E. Alessio, E. Iengo, S. Zorzet, A. Bergamo, M. Coluccia, A. Boccarelli and G. Sava, *J. Inorg. Biochem.*, 2000, **79**, 173.
- 4 T. Giraldi, G. Sava, R. Cuman, C. Nisi and L. Lassiani, *Cancer Res.*, 1981, **41**, 2524.
- 5 T. Giraldi and G. Sava, *Anticancer Res.*, 1981, **1**, 163.
- 6 B. Lippert, *Coord. Chem. Rev.*, 1999, **182**, 263.
- 7 K. J. Boudonck, M. W. Mitchell, L. Nemet, L. Keresztes, A. Nyska, D. Shinar and M. Rosenstock, *Toxicol. Pathol.*, 2009, **37**, 280.
- 8 M. H. Hanigan, D. M. Townsend and A. J. Cooper, *Toxicology*, 2009, **257**, 174.
- 9 K. Negishi, E. Noiri, K. Doi, R. Maeda-Mamiya, T. Sugaya, D. Portilla and T. Fujita, *Am. J. Pathol.*, 2009, **174**, 1154.
- 10 R. Cavaliere and D. Schiff, *Curr. Neurol. Neurosci. Rep.*, 2006, **6**, 218.
- 11 L. Gamelin, O. Capitain, A. Morel, A. Dumont, S. Traore, L. B. Anne, S. Gilles, M. Boisdron-Celle and E. Gamelin, *Clin. Cancer Res.*, 2007, **13**, 6359.
- 12 S. B. Park, C. S. Lin, A. V. Krishnan, D. Goldstein, M. L. Friedlander and M. C. Kiernan, *PLoS One*, 2011, **6**, e18469.
- 13 L. E. Ta, L. Espeset, J. Podratz and A. J. Windebank, *Neurotoxicology*, 2006, **27**, 992.
- 14 G. Cavaletti, G. Nicolini and P. Marmiroli, *Front. Biosci.*, 2008, **13**, 3506.
- 15 E. Chatelut, *Bull. Cancer*, 2011, **98**, 1253.
- 16 P. Heffeter, U. Jungwirth, M. Jakupc, C. Hartinger, M. Galanski, L. Elbling, M. Micksche, B. Keppler and W. Berger, *Drug Resist. Updat.*, 2008, **11**, 1.
- 17 L. P. Martin, T. C. Hamilton and R. J. Schilder, *Clin. Cancer Res.*, 2008, **14**, 1291.
- 18 S. R. McWhinney, R. M. Goldberg and H. L. McLeod, *Mol. Cancer Ther.*, 2009, **8**, 10.
- 19 U. Olszewski and G. Hamilton, *Anticancer Agents Med. Chem.*, 2010, **10**, 293.
- 20 N. Shah and D. S. Dizon, *Future Oncol.*, 2009, **5**, 33.
- 21 B. Stordal, N. Pavlakis and R. Davey, *Cancer Treat. Rev.*, 2007, **33**, 347.
- 22 N. J. Wheate, S. Walker, G. E. Craig and R. Oun, *Dalton Trans.*, 2010, **39**, 8113.
- 23 S. H. van Rijt and P. J. Sadler, *Drug Discovery Today*, 2009, **14**, 1089.
- 24 E. S. Antonarakis and A. Emadi, *Cancer Chemother. Pharmacol.*, 2010, **66**, 1.
- 25 A. Amin and M. A. Buratovich, *Mini-Rev. Med. Chem.*, 2009, **9**, 1489.
- 26 A. Bergamo and G. Sava, *Dalton Trans.*, 2007, 1267.
- 27 V. Brabec and O. Novakova, *Drug Resist. Updates*, 2006, **9**, 111.
- 28 T. Bugarcic, O. Novakova, A. Halamikova, L. Zerzankova, O. Vrana, J. Kasparkova, A. Habtemariam, S. Parsons, P. J. Sadler and V. Brabec, *J. Med. Chem.*, 2008, **51**, 5310.
- 29 A. Bergamo and G. Sava, *Dalton Trans.*, 2011, **40**, 7817.
- 30 C. G. Hartinger, S. Zorbas-Seifried, M. A. Jakupc, B. Kynast, H. Zorbas and B. K. Keppler, *J. Inorg. Biochem.*, 2006, **100**, 891.
- 31 F. Lentz, A. Drescher, A. Lindauer, M. Henke, R. A. Hilger, C. G. Hartinger, M. E. Scheulen, C. Dittrich, B. K. Keppler and U. Jaehde, *Anticancer Drugs*, 2009, **20**, 97.
- 32 J. M. Rademaker-Lakhai, D. van den Bongard, D. Pluim, J. H. Beijnen and J. H. M. Schellens, *Clin. Cancer Res.*, 2004, **10**, 717.
- 33 L. Kersten, H. Braunlich, B. K. Keppler, C. Gliesing, M. Wendelin and J. Westphal, *J. Appl. Toxicol.*, 1998, **18**, 93.
- 34 G. Sava, S. Zorzet, C. Turrin, F. Vita, M. Soranzo, G. Zabucchi, M. Cocchietto, A. Bergamo, S. DiGiovine, G. Pezzoni, L. Sartor and S. Garbisa, *Clin. Cancer Res.*, 2003, **9**, 1898.
- 35 G. Sava, I. Capozzi, K. Clerici, G. Gagliardi, E. Alessio and G. Mestroni, *Clin. Exp. Metastasis*, 1998, **16**, 371.
- 36 G. Mestroni, E. Alessio and G. Sava, Salts of Anionic Complexes of Ru(III), as Antimetastatic and Antineoplastic Agents, WO/1998/000431[US], Sigea S.r.l., Trieste, IT, 1998, 6-30-1997.
- 37 A. Bergamo, R. agliardi, V. carcia, A. urlani, E. Alessio, G. estroni and G. ava, *J. Pharmacol. Exp. Ther.*, 1999, **289**, 559.
- 38 P. E. Kintzel, *Drug Saf.*, 2001, **24**, 19.
- 39 E. Chu and V. T. Devita, in *Physicians' Cancer Chemotherapy Drug Manual*, Jones and Bartlett Publishers, Sudbury, MA, 10th edn, 2010.
- 40 V. Sahni, D. Choudhury and Z. Ahmed, *Nat. Rev. Nephrol.*, 2009, **5**, 450.
- 41 M. Links and C. Lewis, *Drugs*, 1999, **57**, 293.
- 42 M. J. A. de Jonge and J. Verweij, *Semin. Oncol.*, 2006, **33**, 68.
- 43 F. H. Hausheer, H. Kochat, A. R. Parker, D. Ding, S. Yao, S. E. Hamilton, P. N. Petluru, B. D. Leverett, S. H. Bain and J. D. Saxe, *Cancer Chemother. Pharmacol.*, 2003, **52**, 3.
- 44 L. M. Schuchter, M. L. Hensley, N. J. Meropol and E. P. Winer, *J. Clin. Oncol.*, 2002, **20**, 2895.
- 45 M. L. Hensley, K. L. Hagerty, T. Kewalramani, D. M. Green, N. J. Meropol, T. H. Wasserman, G. I. Cohen, B. Emami, W. J. Gradishar, R. B. Mitchell, J. T. Thigpen, A. Trotti, D. von Hoff and L. M. Schuchter, *J. Clin. Oncol.*, 2009, **27**, 127.
- 46 N. Brock, P. Hilgard, J. Pohl, K. Ormstad and S. Orrenius, *J. Cancer Res. Clin. Oncol.*, 1984, **108**, 87.
- 47 M. H. Cohen, R. Dagher, D. J. Griebel, A. Ibrahim, A. Martin, N. S. Scher, G. H. Sokol, G. A. Williams and R. Pazdur, *Oncologist*, 2002, **7**, 393.
- 48 M. Turrill, D. V. Spicer, A. S. Kelley, R. L. Herman, C. A. Russell and F. M. Muggia, *Cancer Invest.*, 1995, **13**, 160.
- 49 I. Khalaila, A. Bergamo, F. Bussy, G. Sava and P. J. Dyson, *Int. J. Oncol.*, 2006, **29**, 261.
- 50 P. J. Dyson and G. Sava, *Dalton Trans.*, 2006, 1929.
- 51 M. I. Webb and C. J. Walsby, *Dalton Trans.*, 2011, **40**, 1322.
- 52 E. S. Antonarakis and A. Emadi, *Cancer Chemother. Pharmacol.*, 2010, **66**, 1.
- 53 L. Messori, P. Orioli, D. Vullo, E. Alessio and E. Iengo, *Eur. J. Biochem.*, 2000, **267**, 1206.
- 54 M. Ravera, S. Baracco, C. Cassino, P. Zanello and D. Osella, *Dalton Trans.*, 2004, 2347.
- 55 M. Bouma, B. Nuijen, M. T. Jansen, G. Sava, A. Flaibani, A. Bult and J. H. Beijnen, *Int. J. Pharm.*, 2002, **248**, 239.

- 56 G. Sava, A. Bergamo, S. Zorzet, B. Gava, C. Casarsa, M. Cocchietto, A. Furlani, V. Scarcia, B. Serli, E. Iengo, E. Alessio and G. Mestroni, *Eur. J. Cancer*, 2002, **38**, 427.
- 57 G. Mestroni, E. Alessio, G. Sava, S. Pacor, M. Coluccia and A. Boccarelli, *Met.-Based Drugs*, 1994, **1**, 41.
- 58 M. Ravera, S. Baracco, C. Cassino, D. Colangelo, G. Bagni, G. Sava and D. Osella, *J. Inorg. Biochem.*, 2004, **98**, 984.
- 59 M. Ravera, S. Baracco, C. Cassino, P. Zanello and D. Osella, *Dalton Trans.*, 2004, 2347.
- 60 M. Bacac, A. C. G. Hotze, K. van der Schilden, J. G. Haasnoot, S. Pacor, E. Alessio, G. Sava and J. Reedijk, *J. Inorg. Biochem.*, 2004, **98**, 402.
- 61 M. J. Clarke, F. Zhu and D. R. Frasca, *Chem. Rev.*, 1999, **99**, 2511.
- 62 N. Cetinbas, M. I. Webb, J. A. Dubland and C. J. Walsby, *J. Biol. Inorg. Chem.*, 2010, **15**, 131.
- 63 F. H. Hausheer, D. Ding, D. Shanmugarajah, B. D. Leverett, Q. Huang, X. Chen, H. Kochat, P. Y. Ayala, P. N. Petluru and A. R. Parker, *J. Pharm. Sci.*, 2011, **100**, 3977.
- 64 M. Verschraagen, E. Boven, E. Torun, C. A. Erkelens, F. H. Hausheer and W. J. van der Vijgh, *Br. J. Cancer*, 2004, **90**, 1654.
- 65 M. Vadori, S. Pacor, F. Vita, S. Zorzet, M. Cocchietto and G. Sava, *J. Inorg. Biochem.*, 2013, **118**, 21.